GIORNALE DI FISICA VOL. LXIV, Passion for Earth 2022 2023
DOI 10.1393/gdf/i2023-10524-5

Spectroscopic measurement of geoneutrinos from uranium and thorium with KamLAND

N. Kawada and the KamLAND Collaboration

Research Center for Neutrino Science, Tohoku University, Sendai, Japan

Abstract. The decays of radioactive isotopes, uranium, thorium and potassium, inside the Earth generate a significant amount of radiogenic heat and contribute to the Earth's heat budget. The abundance of these elements is a key parameter to reveal the planet's geophysical activities. Geoneutrinos originated from these isotopes are a unique probe to the composition, and thus, the amount of the radiogenic heat in the Earth. KamLAND has observed geoneutrinos from ^{238}U and ^{232}Th with 1 kt liquid scintillator for more than 20 years. The low-reactor period since 2011 enabled a spectroscopic measurement of geoneutrinos from ^{238}U and ^{232}Th by reducing the most significant background, which is reactor neutrino. The number of geoneutrino signal is estimated to be $116.6^{+41.0}_{-38.5}$, $57.5^{+24.5}_{-24.1}$ and $173.7^{+29.2}_{-27.7}$ from ^{238}U, ^{232}Th and $^{238}\mathrm{U} + {}^{232}\mathrm{Th}$, respectively. These correspond to a geoneutrino flux of $14.7^{+5.2}_{-4.8}$, $23.9^{+10.2}_{-10.0}$ and $32.1^{+5.8}_{-5.3} \times 10^5\,\mathrm{cm}^{-2}\,\mathrm{s}^{-1}$, respectively. The null-signal hypothesis is disfavored at 8.5σ confidence level. This study yields the first constraint on the radiogenic heat contribution from ^{238}U and ^{232}Th individually, which is consistent with geochemical predictions based on the compositional analysis of chondrite meteorites.

1. Neutrino geoscience

Seismology has shown that our planet has a three-layer structure: crust, mantle and core. Geochemistry has estimated the average composition of the bulk-silicate Earth, *i.e.* crust and mantle, from the composition of chondrite meteorites and reachable rock samples in the Earth. However, because geochemistry predicts the terrestrial composition with hand-sized samples, there is an inherent uncertainty in the compositional estimates by geochemistry. Therefore, a direct test of the Earth's chemical composition is necessary.

The Earth is known to be in a global cooling process. Geodynamical processes, such as plate tectonics and volcanism, are powered by the heat inside the Earth. The surface heat flux is measured by a huge number of bore-hole measurements to be 47 ± 2 TW. The source of this heat is primordial heat and radiogenic heat, while heat flux measurements cannot determine the balance of these heat sources. Radiogenic heat is generated by radioactive elements in the Earth. Once we determine the present amount, we can calculate the past amount of it through the planetary history. So, radiogenic heat is very important for understanding the geothermal evolution of our planet. However, there are different predictions for the radiogenic heat amount from

geophysics and geochemistry. And there is no concensus in geoscience. Therefore, direct measurement is necessary.

Geoneutrino is a key to a direct test of the Earth's interior. In the Earth, uranium and thorium are distributed in crust and mantle. They emit radiogenic heat and elementary particles called geoneutrinos. By measuring the flux of geoneutrinos, we can know the abundance of uranium and thorium, and then we can directly verify the abundance of radiogenic heat inside the Earth. In addition, uranium and thorium have different geoneutrino energies. Therefore, by observing the geoneutrino energy spectrum, we can measure the ratio of uranium and thorium and test the chemical composition of the Earth.

Geoneutrino flux is cacluated from the knowledge of particle physics: neutrino luminosity per decay (A_i), decay rate of uranium and thorium (N_i), and survival probability $P(|\vec{r}-\vec{r'}|)$, and geoscientific parameters: concentration ($a_i(\vec{r'})$) and density ($\rho(\vec{r'})$) of uranium and thorium as per eq. (1) below:

$$\frac{\mathrm{d}\Phi}{\mathrm{d}R} = \sum_{i\in \mathrm{U,Th}} A_i \cdot N_i \int_{\mathrm{earth}} \mathrm{d}^3\vec{r'} \frac{a_i(\vec{r'})\rho(\vec{r'})}{4\pi|\vec{r}-\vec{r'}|^2} P(|\vec{r}-\vec{r'}|) \cdot \delta(|\vec{r}-\vec{r'}|-R). \tag{1}$$

In this study we adopted a reference estimation Enomoto *et al.* [1]. The crust and sediment contribution were calculated based on geochemical studies and cosmochemical studies, such as rock samples and chondrite samples. All the local geological effect was averaged and taken into account in uncertainty calculations. Whereas, the dominant uncertainty came from uranium and thorium concentration measurements. On the other hand, mantle contribution is calculated by subtracting crustal and sedimental contribution from a bulk-silicate Earth compositional model and is not a direct calculation. So this mantle part is the region of interest in this study and we can test this with geoneutrinos.

2. The KamLAND detector

KamLAND is an electron anti-neutrino detector consisting of purified 1 kt liquid scintillator and 1879 photomultiplier tubes. The observation started in 2002. In 2005, the KamLAND detector provided the first evidence of geoneutrino detection, *i.e.* the beginning of neutrino geoscience. The detector has observed geoneutrinos for more than 20 years.

Electron anti-neutrinos are detected via inverse-beta decay channel. When an electron anti-neutrino reacts on a proton, it emits a positron and a thermal neutron. The positron co-anihilates with the electron and makes a prompt scintillation. On the other hand, the thermal neutron is captured by another proton and makes a delayed scintillation. By taking the delayed coincidence of these two scintillations, KamLAND can get an almost background-free anti-neutrino observation profile. This is the primary advantage for KamLAND to measure geoneutrinos. In addition, the

TABLE I. – *The best-fit background model in geoneutrino scan* [3].

	Period 1	Period 2	Period 3	All periods
Live time [day]	1485.5	1151.5	2590.0	5227.0
Reactor $\overline{\nu}_e$	325.75	229.64	48.97	604.36
$^{13}C(\alpha,n)^{16}O$	177.66	20.42	22.18	222.26
Accidental	59.35	40.53	24.79	124.67
Spallation (^{8}He/^{9}Li)	1.52	1.05	1.69	4.26
Background total	620.21	334.07	171.98	1126.26
Observed	651	363	164	1178

TABLE II. – *Best fit and uncertainty of geoneutrino signals* [3].

	$N_{U/Th}$	flux		0-signal rejection
	[event]	[$\times 10^5$ cm^{-2} s^{-1}]	[TNU]	
U	117^{+41}_{-39}	$14.7^{+5.2}_{-4.8}$	$19.1^{+6.7}_{-6.3}$	3.3σ
Th	58^{+25}_{-24}	$23.9^{+10.2}_{-10.0}$	$9.7^{+4.1}_{-4.1}$	2.4σ
U + Th	174^{+31}_{-29}	$32.1^{+5.8}_{-5.3}$	$28.6^{+5.1}_{-4.8}$	8.5σ

incident neutrino energy can be reconstructed from the significance of prompt scintillation. This enables KamLAND to test the geoneutrino energy spectrum. On the other hand, this detection channel does not provide directional information. Therefore, electron anti-neutrinos from commercial reactors (reactor neutrinos) are the dominant background for geoneutrino observation.

The reactor-dominant situation drastically changed in 2011. Due to a huge earthquake in east Japan, most of Japanese reactors have been shut down. This "reactor-off" period significantly suppressed the reactor neutrinos background and improved the signal-to-noise ratio of geoneutrino observation in Japan. This presentation is the first report of geoneutrino measurement using the reactor-off period in Japan.

3. Best-fit geoneutrino signals

The flux, or amount, of geoneutrino signals was determined by a spectrum fitting using energy and time information acquired in KamLAND. Besides, since the reactor neutrinos spectrum depends on oscillation parameters, simultaneous scans of the oscillation parameters, non-neutrino backgrounds and geoneutrinos are performed. The best-fit energy spectra of geoneutrino signal and backgrounds are summarized in table I, table II and fig. 1.

The dataset is divided into three periods. From period 1 to period 2, the $^{13}C(\alpha,n)^{16*}O$ background was significantly suppressed. This $^{13}C(\alpha,n)^{16*}O$ reaction

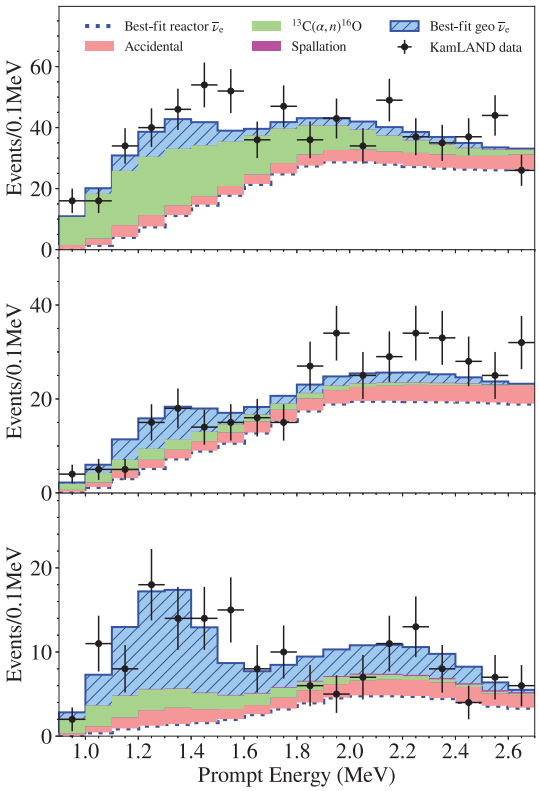

Fig. 1. – Energy spectrum in period 1 (top), period 2 (middle) and period 3 (bottom). This figure is cited from [2].

is triggered by α activity in the detector, makes two correlated scintillations and mimics an inverse-beta decay signal. According to [4], the dominant α activity in the KamLAND liquid scintillator is ^{210}Po, which is produced by radioactive equilibrium of ^{210}Pb. To remove ^{210}Pb from the liquid scintillator, two distillation campaigns were performed in 2007 and 2008, which is the boundary between period 1 and period 2. As a result of the distillation, the $^{13}C(\alpha,n)^{16*}O$ background was significantly suppressed and almost negligible in period 2 and period 3. The boundary of period 2 and period 3 is in 2011, that is, period 3 is the reactor-off period. In period 3, reactor neutrino background was significantly suppressed by the reactor-off environment. In addition, accidental-coincidence background is also supressed by optimization of likelihood-based anti-neutrino event selection in the reactor-off period [3]. Only in period 3, the spectrum shape of the geoneutrino signal is clearly seen: 0.9–1.6 MeV sharper peak as ^{232}Th geoneutrinos and 0.9–2.6 wider peak as ^{238}U geoneutrinos.

As shown in the column "0-signal rejection" of table II, KamLAND detected significant geoneutrino signals from both ^{238}U and ^{232}Th inside the Earth. As discussed in [3], the visibility of the geoneutrino spectrum and the outstanding statistical power of reactor-off period contributed to the determination of geoneutrinos from ^{238}U

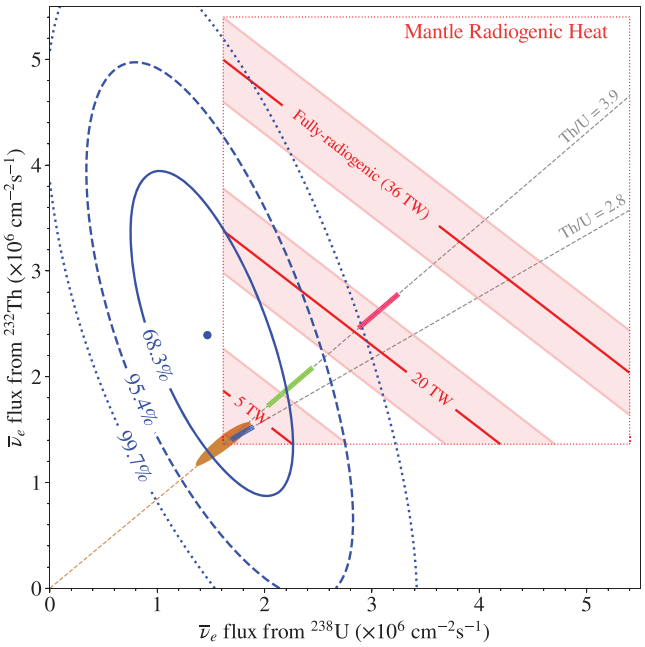

Fig. 2. – Confidence level contour of geoneutrino flux measured by KamLAND (blue circles) with crustal contribution estimated by [1] (brown ellipse), corresponding mantle radiogenic heat (red contour) and radiogenic heat prediction by some bulk-silicate Earth models (blue, green and red bars). This figure is cited from [2].

and ^{232}Th. That is, a spectroscopic measurement of geoneutrinos from uranium and thorium was achieved.

4. Radiogenic heat measurement and Earth models

The confidence level contour of the geoneutrino flux measured by KamLAND is drawn in fig. 2. The flux at the surface is divided into crust contribution and mantle contribution. The crust contribution is calculated in advance [1] and shown as a brown ellipse with uncertainties [5,6]. The mantle contribution is calculated by subtracting crust contribution, $\Phi^{\mathrm{U,Th}}_{\mathrm{crust}}$, from the measured flux, $\Phi^{\mathrm{U,Th}}$, and then converted into the amount of radigenic heat from ^{238}U and ^{232}Th in the mantle, $Q^{\mathrm{U,Th}}_{\mathrm{mantle}}$, using the following eq. (2):

$$Q^{\mathrm{U,Th}}_{\mathrm{mantle}} = \left(\Phi^{\mathrm{U,Th}} - \Phi^{\mathrm{U,Th}}_{\mathrm{crust}}\right) \frac{\mathrm{d}Q^{\mathrm{U,Th}}_{\mathrm{mantle}}}{\mathrm{d}\Phi^{\mathrm{U,Th}}_{\mathrm{mantle}}}, \tag{2}$$

where $\frac{\mathrm{d}Q^{\mathrm{U,Th}}_{\mathrm{mantle}}}{\mathrm{d}\Phi^{\mathrm{U,Th}}_{\mathrm{mantle}}}$ is the conversion coefficient between flux and radiogenic heat in the mantle. The mantle radiogenic heat corresponding to the geoneutrino total flux is

shown as red contours in fig. 2. The bands incorporating the red contours imply a conversion uncertainty due to the uncertainty of crust contribution.

There are different bulk-silicate Earth composition models based on different rationale that predict different amounts of radiogenic heat, as shown in fig. 2 with blue, green and red bars. The blue and green bars are "Low-Q" and "Middle-Q" models, predicting 10–15 TW and 17–22 TW of radiogenic heat, respectively. These models are cosmochemical or geochemical approaches based on compositional analysis of different types of chondrite meteorites, and are consistent with the KamLAND data. On the other hand, the red bar is a "High-Q" model, which is motivated by a geodynamical approach based on seismology, and balancing mantle viscosity and heat dispersion. This model is obviously incompatible with the KamLAND data. The tension between the High-Q model and the KamLAND data is evaluated to be 99.76% with assuming homogeneous mantle composition [3]. Even if we assume uranium and thorium concentration at the mantle-core boundary, this model is disfavored at 97.9%. Given the rationale for the High-Q model, this suggests that we need to modify our understanding of the mantle density/viscosity profile derived from seismology, or geodynamic modeling of mantle convection.

References

[1] Enomoto S. *et al.*, *Earth Planet. Sci. Lett.*, **258** (2007) 15.
[2] Abe S. *et al.*, *Geophys. Res. Lett.*, **49** (2022) e2022GL099566.
[3] Kawada N., *Spectrosopic measurement of geoneutrino from uranium and thorium with KamLAND* (Doctral Dissertation), Tohoku University (2022).
[4] Ichimura K., *Precise measurement of neutrino oscillation parameters with KamLAND* (Doctral Dissertation), Tohoku Univeristy 2008.
[5] Rudnick R. L. and Gao S., *Treatise on Geochemistry: Composition of the Continental Crust*, Vol. **3** (Pergamon Press) 2014.
[6] Wipperfurth S. A. *et al.*, *Earth Planet. Sci. Lett.*, **498** (2018) 15.